Description of ionospheric disturbances observed by Vertical Ionospheric Sounding at 3 MHz

James A. Baskaradas[1], Silvio Bianchi[2], Marco Pietrella[1], Michael Pezzopane[1], Umberto Sciacca[1,*], Enrico Zuccheretti[1]

[1] *Istituto Nazionale di Geofisica e Vulcanologia, Rome, Italy*

[2] *Università "La Sapienza", Dipartimento di Fisica, Rome, Italy*

ABSTRACT

High Frequency radio waves reflected by the ionosphere can provide a relevant amount of information within the composite received signal. The ionosphere is indeed a frequency dispersive, bi-refractive, absorbing medium, in which multipath propagation occurs due to disturbance on a varied time-spatial scale. On the time-spatial level of Small Scale Disturbances (SSD) the ionosphere dynamics, detectable by Vertical Ionospheric Sounding (VIS), is mainly dependent on wrinkled layers acting as multi-reflectors. The present paper discusses different aspects of the effects of multipath fading suffered by the wave along the propagation path and potentially associated with SSD. To achieve these objectives, a VIS campaign at a fixed frequency of 3.0 MHz was conducted at the ionospheric observatory in Rome (Latitude 41.8 N; Longitude 12.5 E), by collecting a series of measurements of the power variations in received echo signals recorded between two consecutive ionograms whose sounding repetition rate was set to 15 min. The obtained results show that: 1) the fading suffered by the wave follows either a Rayleigh trend or a Nakagami-Rice trend, or a mix of them, the mixed case being the most frequent (about 65 % of the analysed cases); 2) the predominant periodicities characterizing the power variation are less than 25 s; such values are compatible with the small scale ionospheric disturbances; 3) for all the 24 hours of the day the ionospheric reflector is pretty stable and for time intervals of 10-30 s the periods of stability occur with a percentage of occurrence ranging between 55% and 95 %; for time intervals of 190- 210 s the periods of stability occur instead with a percentage of occurrence ranging between 5% and 54 %.

1. Introduction

Vertical Ionospheric Sounding (VIS) is a consolidated technique that was first applied nearly a century ago to unveil the existence of the ionosphere, i.e. the density and altitude of the ionospheric layers. It is still widely applied and generates the largest ionospheric parameter database [Reinisch and Galkin 2011]. This technique relies on reflection of radio waves from ionospheric plasma exhibiting plasma frequencies equal or higher to the radio frequencies employed for radio sounding. The VIS technique uses radio waves propagated in the High Frequency (HF) range and reflected by the ionospheric layers acting like mirrors, with the corresponding echo delay related to the reflection virtual height of the reflecting layers.

Nowadays advanced digital sounders are used in the VIS technique for observations that provide detailed information about the structure and dynamics of the bottom side ionosphere. The underlying concepts of the technique remain the same, but modern sounders measure more than just the travel time and amplitude of the echoes. In a measurement campaign, the AIS-INGV (Advanced Ionospheric Sounder - Istituto Nazionale di Geofisica e Vulcanologia) ionosonde, with minor modifications and calibrations, was adapted to measure only Power in dBm and Virtual Height in km (PVH), at a fixed frequency, assuming that the critical frequency and reflection altitude of the ionospheric layers to be investigated were known from routine VIS measurements [Bianchi et al. 2013a]. The latter is important because only starting from this knowledge the PVH measurements can be usefully conducted. Consequently, it is possible to measure the level of received power in nearly controlled conditions, evaluating only certain echo signal characteristics.

In the VIS technique the emitted pulses are reflected back in a mirror-like way if the frequency of the radio waves is lower than the critical frequency, simplifying the propagation path and other relevant parameters. When operating at a fixed frequency, the VIS technique highlights variations in the electron density and virtual heights of the iso-density surfaces, based on the amplitude and

phase analyses of the echo signal. However, single mirror-like reflections are seldom observed in VIS measurements, while dominant multi-reflectors are more probable, following either Rayleigh or Ricean trends, characterized by a single dominant reflector with other less relevant contributions [Bianchi et al. 2013b]. This happens because ionospheric disturbances on a variable time-spatial scale can tilt the ionosphere and corrugate the bottom layer, producing peculiar reflecting characteristics. Moreover, these irregularities travel at different horizontal and vertical velocities, as reported in literature [Leitinger and Rieger 2005, Crowley and Rodrigues 2012].

The moving reflectors introduce a further complication, making the propagation path time variant. Echo signals reflected from the ionosphere and measured by the VIS technique are subject to a degree of variability, according to the traveling irregularities on the small, medium, and large scale [Blanc 1985, Krasnov et al. 2006]. The presence of traveling irregularities in the ionosphere causes the phase difference between different paths vary over time, with consequent time variable signal fading, from a few seconds to tens of seconds. The power signal variations at the receiver input match the time-spatial scale of the irregularities. Due to multipath, different paths can interfere constructively or destructively at the receiving point depending on the phase of the wave components. Among the periodicity times, this paper addresses the ones related to Small Scale Disturbances (SSD), which are characterized by random processes, by exploiting PVH measurements. The narrow band signal propagating in the ionosphere here analyzed was modelled by Rice [1944], Nakagami [1960], and Watterson et al. [1970], and the corresponding temporal power variations have recently been investigated by Bianchi et al. [2013a] by using PVH measurements.

Depending on the position and the shape of the irregularities, the ionosphere acts like convex-concave mirror for HF waves. When radio waves are reflected from a concave iso-density surface, the waves will undergo a focusing gain; conversely when the surface is convex there is a loss due to the defocusing effect. The latter phenomenon, together with multipath fading, defines the behavior of the ionospheric irregularities considered in this paper, where a series of measurements of radio echo power were performed to study and monitor some dynamic characteristics of the ionospheric propagation path and related reflecting layers potentially associated with SSD.

2. Experimental setup and measurement campaign

The vertical ionospheric sounding system used for this study was derived from a phase coded HF radar [Bianchi et al. 2003] with the purpose of studying the ionospheric fading under definite controlled conditions. A single fixed frequency PVH sounding, lasting a few minutes, was carried out between two consecutive vertical ionospheric soundings. The inspection of these two ionograms, whose sounding repetition rate was set to 15 minutes, is important to be sure that the investigated ionospheric layer is present and falling in the flat part of the ionogram trace corresponding to the base of the F region (see Figures 1 and 2).

The PVH sounding was performed using the AIS-INGV ionosonde [Zuccheretti et al. 2003], employing complementary phase code of 16 chips, which is a low power HF radar based on the pulse compression technique with a mathematical processing gain of 25 dB; about 13 dB derive from the correlation process while the remainders are related to coherent integration [Bianchi et al. 2013a]. The system records pairs of data: power in dBm and virtual height in km are given for the highest signal peak returning from the ionosphere, and previous calibration allows determination of the correct values.

The system employs low gain, long wire, cross coupled delta antennas with a beam angle of about 60 degrees. This seems a limiting factor, but by applying a range gating function, a limited portion of the reflecting layer can be selected, making it possible to study a return echo signal from a known ionospheric region. Range gating can filter off the unwanted off vertical echoes and noise out of the selected time interval when the receiver is active. The environmental noise always present is instead characterized by an average level of 30 dB lower than the strongest signal peak. For this purpose a session of PVH measurements lasting 512 s were performed in alternation with the normal soundings, lasting approximately 180 s.

The integration time used to increase the signal to noise ratio should be relatively small so that the ionosphere can be assumed stable within the measurement interval. Therefore in order to obtain a good quality signal from the ionosphere, pulses at a rate of 60 Hz were considered, providing after 30 integrations a PVH measurement every 0.5 s.

Figure 1 shows how the power peak (Figure 1b) of the received echo at the frequency f = 3.0 MHz is related to the routine vertical ionograms recorded before (Figure 1a) and after (Figure 1c) the PVH measurement session.

In the illustrated case the virtual height of the layer is at 200 km (Figure 1a,c), and the corresponding position of the power peak recorded during the PVH measurement is shown in Figure 1b. As the PVH measurement session lasts 512 s and the integration time chosen is 0.5 s, the correlation process generates 1024 narrow peaks (see Figure 1b) clearly emerging
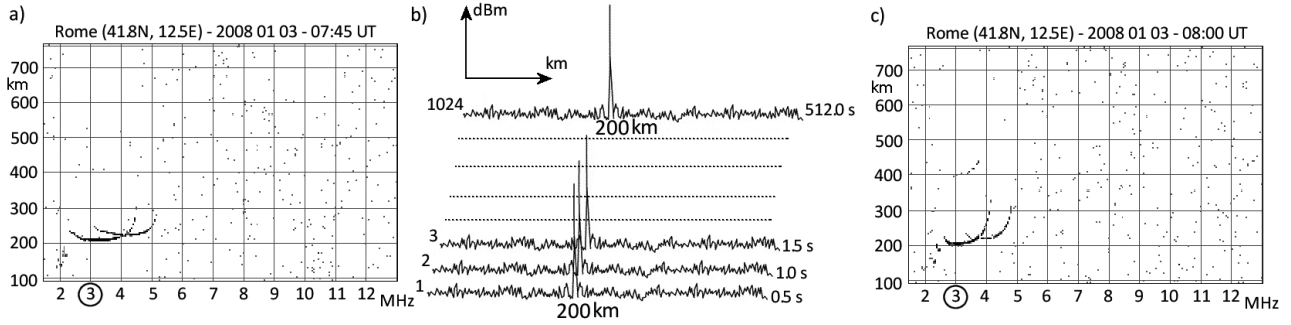
Figure 1. Ionograms recorded by VIS (a) before and (c) after the (b) PVH measurements of the received echo every 0.5 s at the frequency $f = 3.0$ MHz - highlighted by an open circle in (a) and (c). The ionogram sounding repetition rate is 15 minutes. The PVH measurement session lasts 512 s, which corresponds to 1024 samples of PVH.
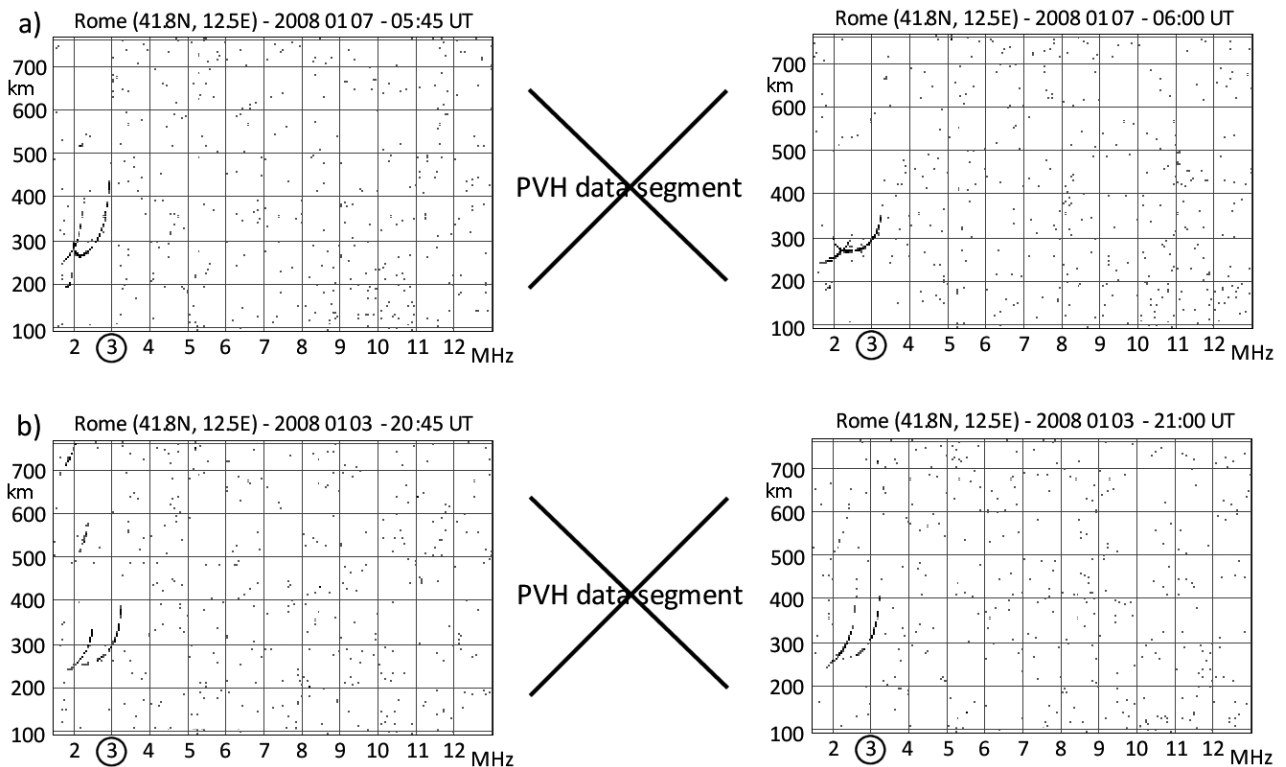
Figure 2. Cases for which the inspection of the two consecutive ionograms helped the data analyzer in discarding the corresponding PVH data segment because: (a) the maximum reflected frequency of the first ionogram is below the value of 3.0 MHz (highlighted by an open circle and corresponding to the PVH operating frequency); (b) the PVH operating frequency propagates up to the highest ionospheric layers and this fact prevents from neglecting the polarization losses (see Section 3).

from the noise level and corresponding to the ionospheric reflectors with an accuracy of about ±0.5 dB for the power and ±5 km for the virtual height .

Figure 2 shows instead two cases for which the inspection of the two consecutive ionograms helped the data analyzer in discarding the corresponding PVH data segment. Figure 2a shows that the ionogram recorded just before the PVH measurement shows a maximum reflected frequency below the value of 3.0 MHz, which is right the PVH operating frequency. Figure 2b shows instead that the PVH operating frequency would deeply penetrate the plasma, up to heights of the F region critical frequency; these PVH data segments were

discarded because in these conditions the polarization losses could be no more neglected (see Section 3).

PVH measurements were performed at the ionospheric observatory of Rome (Italy, 41.8 N, 12.5 E), collecting a series of data during the period from January 3 to 22, 2008. Over the measurement campaign 1920 sequences of PVH 512 s data segments were acquired. The environmental noise level was also analyzed during all the hours of the day in the campaign period, considering that the band of the receiving section is about 66 kHz. The noise resulted approximately around −94 dBm, with the signal ranging from this level up to −64 dBm.

As it will be seen in the next paragraph, it is possi-
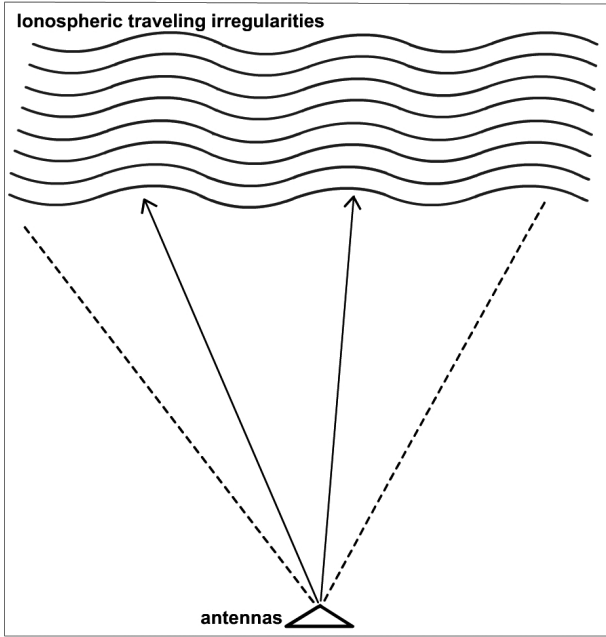
Figure 3. Multi-reflectors produced by traveling irregularities. Signals off vertical represented by dashed line are filtered out by the range gating threshold of the receiver.

ble to ignore the term of the frequency shift in the analytic description. This fact is due to the peculiar condition of the near vertical Line Of Sight (LOS), as inferred from Figure 3 [Crowley and Rodrigues 2012]: only the paths received off-vertical could be affected by a Doppler effect due to the horizontal drift of the layer, but they can be easily cut-off by means of a proper range gating. For example, applying a gating of 10 km, if the height is 100 km, the area of the ionospheric layer actually investigated is some hundreds of square km.

3. Analytic signal characterization in a multipath time-varying propagation path

The signal at the receiving point is the sum of the multipath components generated by the irregularities in the ionosphere. Each path is subject to several attenuating factors as shown in Table 1.

Considering Table 1, partially derived from [McNamara 1991], it is important to establish which terms are approximately constant and which terms vary in the observed excursion range under the experimental conditions of PVH measurements. This makes it possible to measure the level of received power in nearly controlled conditions and evaluate specific contributions. The complete mathematical expression of the received echo signal is expressed by the following relation:

$$r(t) = \sum_{i=0}^{M} \alpha_i(t) \cdot u(t - \tau_i(t)) \cdot$$
$$\cdot \cos\{2\pi f_0[t - \tau_i(t)] + \varphi_i(t)\} + N(t) , \quad (1)$$

where t is the time, $r(t)$ is the sum of time delayed attenuated frequency shifted replica of the emitted signal with envelope $u(t)$ containing the bi-phase code, M is the number of paths, dependent on time, $\alpha_i(t)$ is the attenuating factor of the i-th path (it assumes values from 0 to 1, taking into account all the loss contributions given in Table 1), $u(t-\tau_i(t))$ is the received waveform, $\tau_i(t)$ is the time dependent delay, f_0 is the carrier frequency, $\varphi_i(t)$ is the phase, dependent on the time delay $\tau_i(t)$, and $N(t)$ is the noise [Bianchi et al. 2013a].

When the layers move the signal can experience a Doppler frequency shift that changes the phase according to $2\pi f_0[d\tau_i(t)/dt] \cdot t$, approximating to the first order of the Taylor series expansion. This latter term is ignored in the present paper together with the term $\varphi_i(t)$ because of their irrelevant contributions to the power variation of the signal. Given that in this context only variations in the time interval of 512 s are important, that is those related to SSD, the impulsive noise is mitigated by the integration process and has less effect on the overall signal power.

With these assumptions, the echo signal is then down converted to the baseband as described in the following relation:

Loss in the ionospheric propagation path	In PVH measurement	Typical values (dB unit)
Free space loss (L_g)	$\approx$ Constant	50-150
Ionospheric absorption (L_a)	$\approx$ Constant	0-20
Ionospheric deviative absorption (L_d)	$\approx$ Constant	<1
Scattering (L_s)	$\approx$ Constant	<1
Differential Doppler (L_D)	$\approx$ Constant	0.5
Blanketing sporadic E (L_E)	$\approx$ Constant	0-1
Polarization losses (L_p)	$\approx$ Constant	3-6
Focusing losses (L_f) (negative = gain)	Not Constant	$\pm$0-1
Multipath losses (L_m)	Not Constant	0-25

Table 1. Loss contributions in the PVH ionospheric propagation path.

$$y(t) = \sum_{i=0}^{M} \alpha_i(t) \cdot u(t - \tau_i(t)) . \qquad (2)$$

This is the attenuated composite envelope signal whose components have different times of arrival (multipath components), with different phases interfering in constructive or destructive ways.

The attenuating terms in Table 1 are carefully evaluated individually in the limited condition of VIS operating at a fixed frequency. The free space loss L_g as well as the ionospheric absorption L_a are practically constant because of the range gating that excludes longer or shorter paths, and the 3.0 MHz frequency wave does not penetrate deeply into the plasma, being it often reflected by the flat part of the ionogram trace corresponding to the base of the F region. The terms L_d, L_s, L_D, have the values indicated in Table 1, assumed as constants. Concerning the L_E loss, the presence of the Es layer is rare, or at least during the measurements. Polarization losses L_p [James et al. 2006] are not considered since in the considered PVH measurements the low frequency employed does not deeply penetrate the plasma (see Figures 1 and 2). For the same reason Faraday rotation is ignored while in general this fading can produce a loss from 0 to a few dB units. Considering the irregular time changing contours of the iso-density surfaces, statistically it is rare to have only one flat reflector. On the contrary, reflectors with a convex-up or concave-up shape and producing respectively further gain or loss to the signal can be expected [Bianchi et al. 2003]. These are the focusing losses L_f that in the selected experimental conditions do not exceed $\pm$ 1 dB. In the constraints given by VIS the experimental multipath losses L_m is the only term that really produces deep fading on the echo signal.

4. Data analysis and results

This paragraph presents different ways of expressing the results in terms of radio electric parameters from different physical points of view of the effects of the SSD. The SSD undulate the reflecting iso-density surfaces, producing multipath echoes and making different reflection sources possible. From the power variation of the echo signal potentially associated to SSD and observed in the VIS technique, three main phenomena have been studied and described in the following paragraphs. In Table 2 the main features of the SSD and the other types of TIDs are summarized, so that it is possible to compare the corresponding horizontal scales (L) of the irregularities, the period (T), the phase velocity and the characteristics of the associated fading.

4.1. Trends of the signal

The ionospheric propagation path exhibits different trends, according to whether there is a dominant single reflector or multiple reflectors, inferred by the power variation in time of the echo signal. The received power ranges approximately from −64 to −97 dBm, with an excursion of ≈ 33 dB over the various hours of the day. The same peculiar trends, Rayleigh or Nakagami-Rice, within the same hour or from hour to hour, were observed in the acquired 512 s time-sequences of the signal. As an example, Figure 4 shows one of the time sequences recorded showing a well defined Rayleigh trend. In this case a large number of reflecting sources are contributing to the composite signal.

The two trends have different peak amplitudes (note the different scale between Figures 4 and 5) even if the time periodicity does not differ to a significant degree. In general, the most common trend we obtained (65% of the considered PVH time sequences) is the mixed case Nakagami-Rice and Rayleigh as in Figure 6.

In general, it is possible to state that SSD cause multi-reflections showing a trend, except in some particular ionospheric conditions. Figure 7a,b shows the results of the FFT analysis of the temporal sequences shown in Figures 4 and 5 respectively for Rayleigh and Nakagami-Rice trends. They show the typical power density behavior and the spectral content of the two sequences. It can be observed that the Rayleigh behavior

| Scale-irregularities	L (km)	T (min)	Phase velocity (m/s)	Associated fading
SSD: Small-Scale Disturbances (infrasonic variability)	< 100	< 10	< 50	Multipath fading - Less relevant focusing /defocusing phenomena
MSTID: Medium-Scale Traveling Ionospheric Disturbances	100 - 300	10 - 30	50 - 300	Amplitude fading - Focusing / defocusing phenomena
LSTID: Large-Scale Traveling Ionospheric Disturbances; Acoustic Gravity Waves	300 - 3000	30 - 300	300 - 1000	Amplitude fading - Focusing / defocusing - Deep fading due to ionospheric tilt

Table 2. TID classes according to their horizontal scales derived from Crowley and Rodrigues [2012].
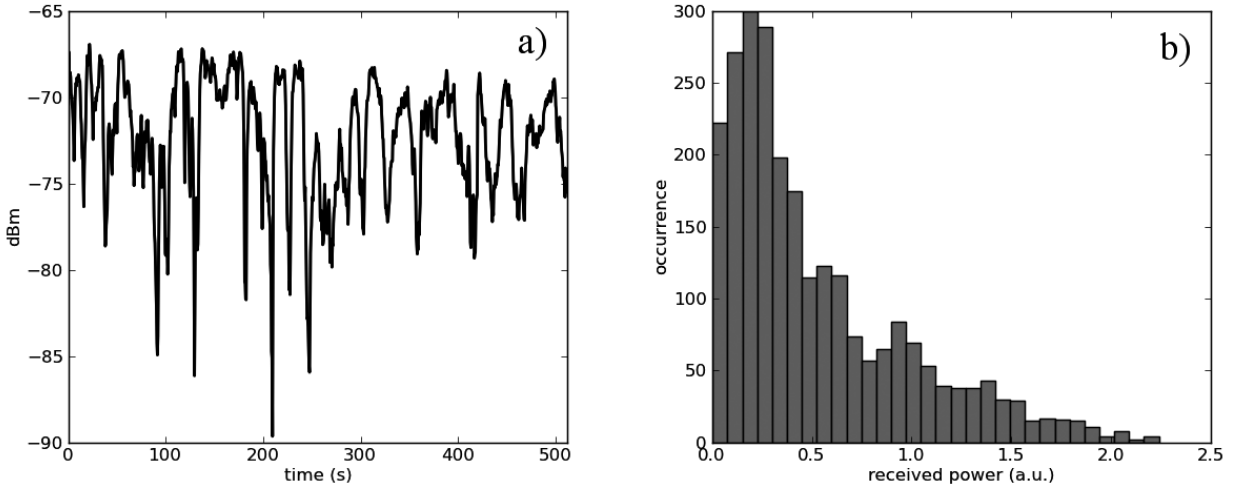
Figure 4. (a) Power observations of the radio echo reflected from the ionosphere on January 7, 2008, at 12:25 UT; (b) corresponding Rayleigh probability density distribution.
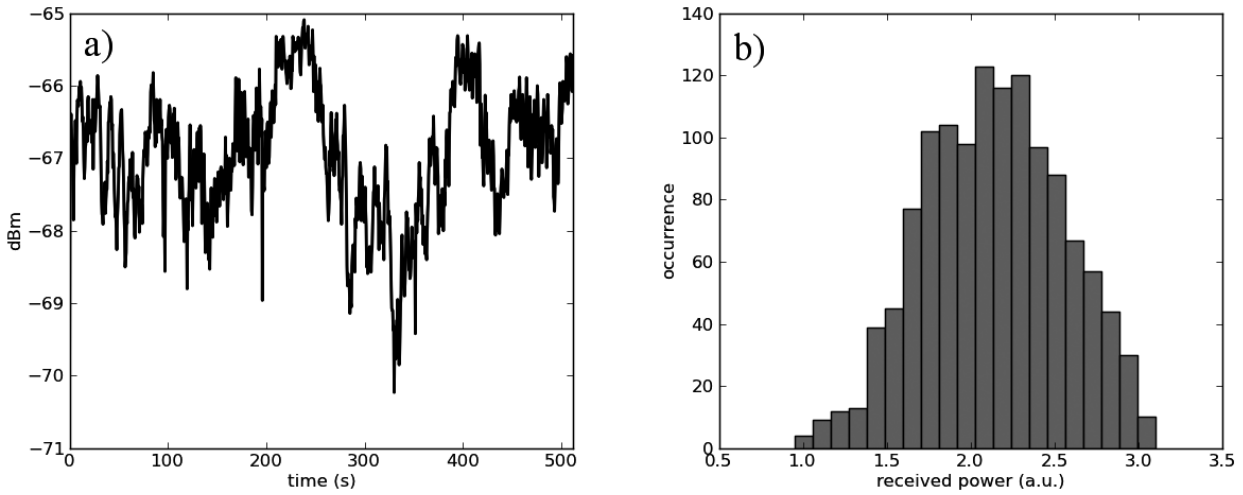
Figure 5. (a) Power observations of the radio echo reflected from the ionosphere on January 13, 2008, at 07:40 UT; (b) corresponding Nakagami-Rice probability density distribution.
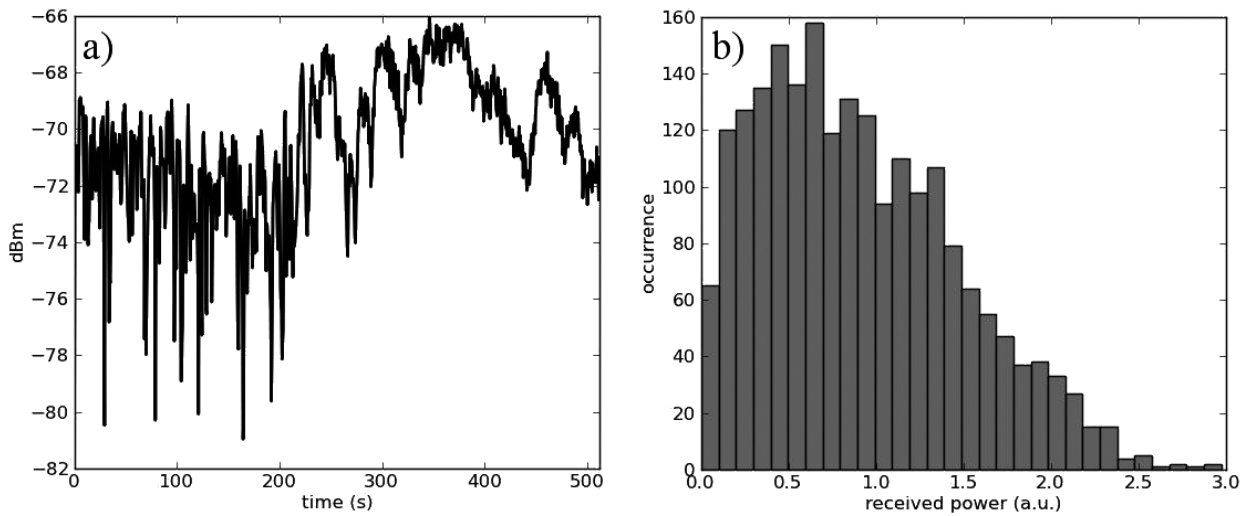
Figure 6. (a) Power observations of the radio echo reflected from the ionosphere on January 7, 2008, at 19:55 UT; (b) corresponding mixed behavior Rayleigh -Nakagami-Rice probability density distribution.

has a higher spectral content at lower frequencies with respect to Nakagami-Rice. Figure 7c highlights the two trends as a result of a 100-values running mean performed on the spectral density sequences of Figure 7a,b.

### 4.2. Effects of SSD on signal fading

As regards the excursion of power variation, it was often observed that a few tens of dBm is not rare, especially when ionospheric tilts or large scale disturbance are present. As an example in this context, considering only the SSD, two almost consecutive 210 s sequences of signal, are shown in Figure 8 (power vs. time). It is possible to note completely different fading characteristics.

Either periodicities or power excursion values can change rapidly during the observation time periods. The power variation imposed by the ionospheric disturbances causes multipath fading in an unpredictable way at different time intervals. It was however observed that short time periodicities are much more frequent compared to longer periodicities (Figure 9). Nevertheless, this does not exclude longer time periods compatible with MSTID and LSTID, but these were not considered in the present analysis. However, by and large, these results suggest that the observed power and periodicity excursions are potentially caused by small time-spatial scale disturbances compatible with SSD, as illustrated in Table 2. Finally, it is worth noting that this phenomenology is a characteristic of the normal ionosphere, that is it is not caused by high levels of the geomagnetic activity.

4.3. Effects of SSD on coherence time

The time variant propagation path affects the performances of systems that have to rely on stability of the ionospheric reflector for at least some tenths of a second. These include Over the Horizon Radar (OTHR) and other remote sensing applications that exploit ionospheric reflections. Some HF communication systems employing broader band techniques can also be affected by time propagation path variation. In other terms, these systems need to exploit the stability of the propagation path to establish the Coherent Integration Time (CIT). The VIS technique also relies on this mathematical process, integrating the received echo signal for the necessary time under stable conditions [Yau et al. 2006, Bianchi et al. 2013a].

In order to determine stability periods, a software program [Pietrella and Zuccheretti 2010], capable to elaborate the data of the whole measurement campaign, was employed. This software uses a statistical parameter to identify time periods of maximum signal stability over time. The term "maximum ionospheric stability intervals" is used here to refer to periods of time during which the ionosphere does not exhibit significant dynamic changes, which means that the signal power will range within the values to be established according to the criteria described below. Standard deviation proved to be an appropriate parameter for
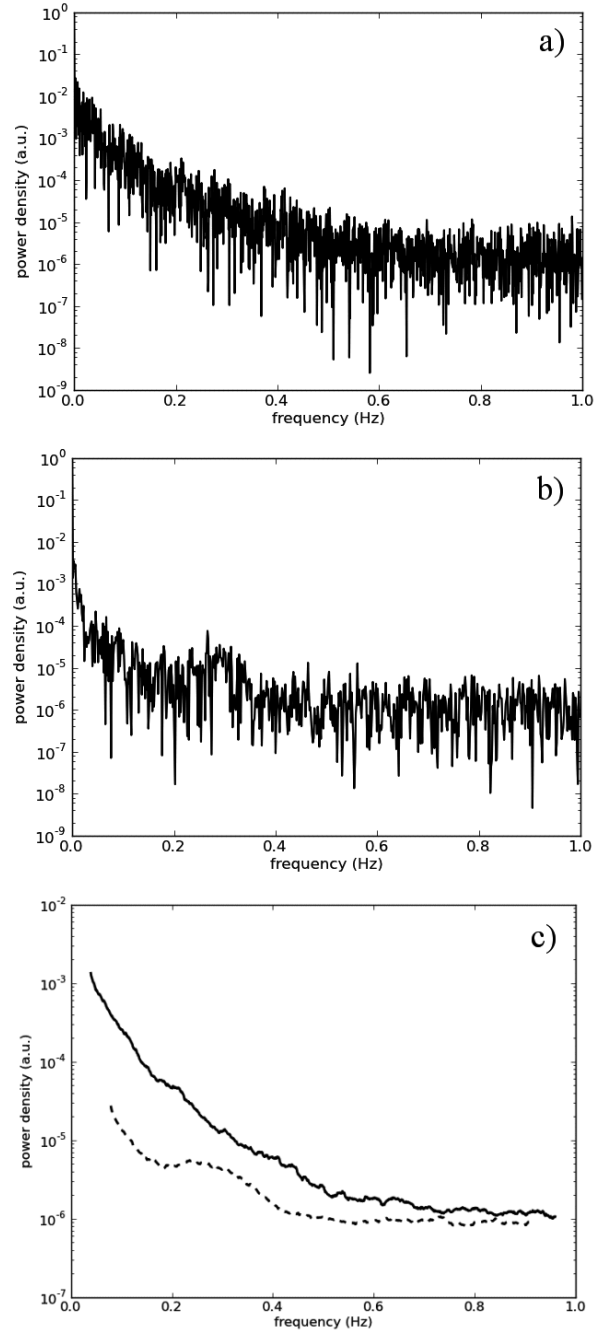
Figure 7. FFT spectral analysis (log of power density vs. frequency) of the (a) Rayleigh and (b) Nakagami-Rice behavior shown in Figures 4 and 5 respectively. (c) FFT Comparison between the Rayleigh (continuous curve) and Nakagami-Rice (dashed curve) behavior obtained by doing a 100-values running mean of the values plotted respectively in (a) and (b).

quantifying the dispersion of power values and altitude, since it is an index of dispersion, i.e. a measurement of variability of a random variable around a central value. Therefore, standard deviation of power (σ_{dBm}) and of virtual height ($\sigma_{h'}$) identify periods in which the observed variation data are not significant; in such cases the ionosphere can be considered stable. For each PVH data segments, subsets of different duration, from 10 to 210 s, can be selected and the standard deviation σ_{dBm} and $\sigma_{h'}$ can be calculated. Reduced σ_{dBm} and $\sigma_{h'}$ values
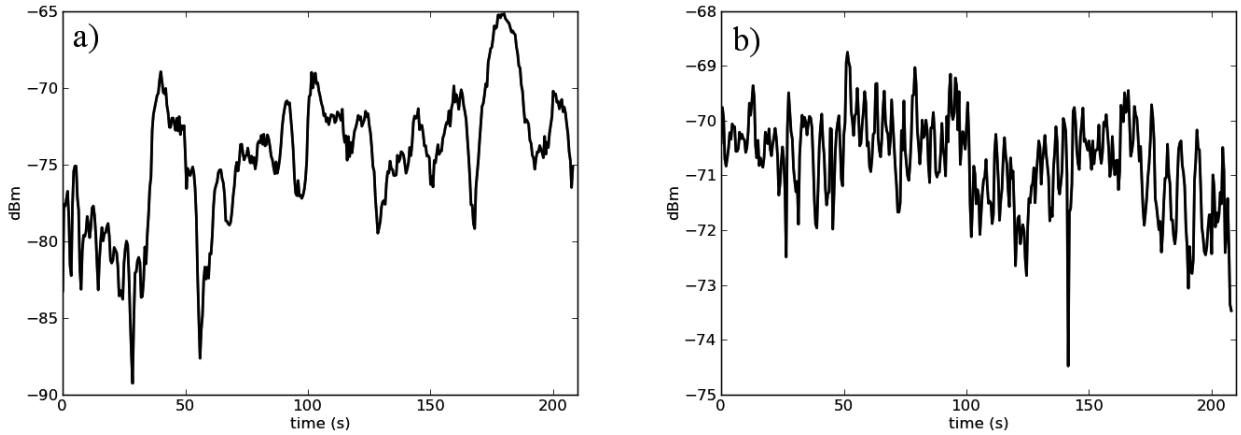
Figure 8. Power observations of two almost consecutive data segments of 210 s showing different fading levels and different periodicities recorded on January 14, 2008, at (a) 06:55 UT and (b) 07:55 UT respectively.

result in greatly reduced power and virtual height variations for the period considered. Consequently, choosing the threshold values T_{dBm} and $T_{h'}$, the conditions:

$$(\sigma_{dBm} < T_{dBm}) \text{ AND } (\sigma_{h'} < T_{h'}) \tag{3}$$

can be assumed as the criteria to identify the stability through time of the ionospheric propagation path. Applying criterion (3) the maximum duration of stability were calculated [Bianchi et al. 2013a].

In order to obtain an overall view, representative of the stability through time of the reflected ionospheric echoes, all the 24 hours of the entire measurement campaign were analyzed. As expected, it was found that the number of time periods of stability are generally less frequent at dusk and dawn compared to night and day. Some relevant percentages of occurrence
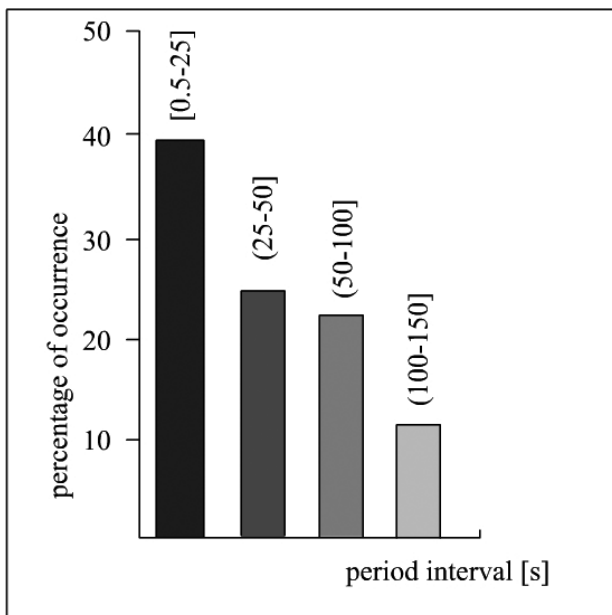
calculated by means of (3) are reported as a bar histogram for each hour in Figure 10, which shows the results for stability over the time interval 10-30 s using a threshold of $T_{dBm} = 1$ dBm and $T_{h'} = 5$ km. In this case the periods of stability occur with a percentage of occurrence ranged between 55-95 %.

The analysis results carried out to identify longer stability time periods from 190 to 210 s are reported in Figures 11 and 12. When this longer time period is required, the ionospheric layers rarely reveal a stability within the restrictive threshold of 1 dBm and 5 km (Figure 11).

By relaxing the threshold values to 5 dBm and 10 km, an higher percentage of occurrences ranged between 5-54 % is found (Figure 12).

It is worth noting that these kind of analyses are often considered for OTHR applications aimed to target detection.

5. Conclusions

The study described in this paper had three main objectives: to study the effect of small time-spatial scale irregularities on the ionospheric propagation path, multipath fading, and determination of the time stability characterizing the coherence time of the ionospheric reflectors. These three issues derive from the same unpredictable phenomena, which are the small scale disturbances propagating in the ionosphere.

A first aspect that emerges from the analysis is the behavior of the ionospheric channel, which can show a Rayleigh or a Nakagami-Rice trend, or a combination of them. The latter could be applicable for characterizing models for ionospheric propagation path simulators. Another aspect is the analysis of the deep fading fluctuations due to ionospheric time-variant propagation path behavior. This permits the identification of a series of ionospheric characteristics varying in time and potentially related to the SSD phenomena. A third as-
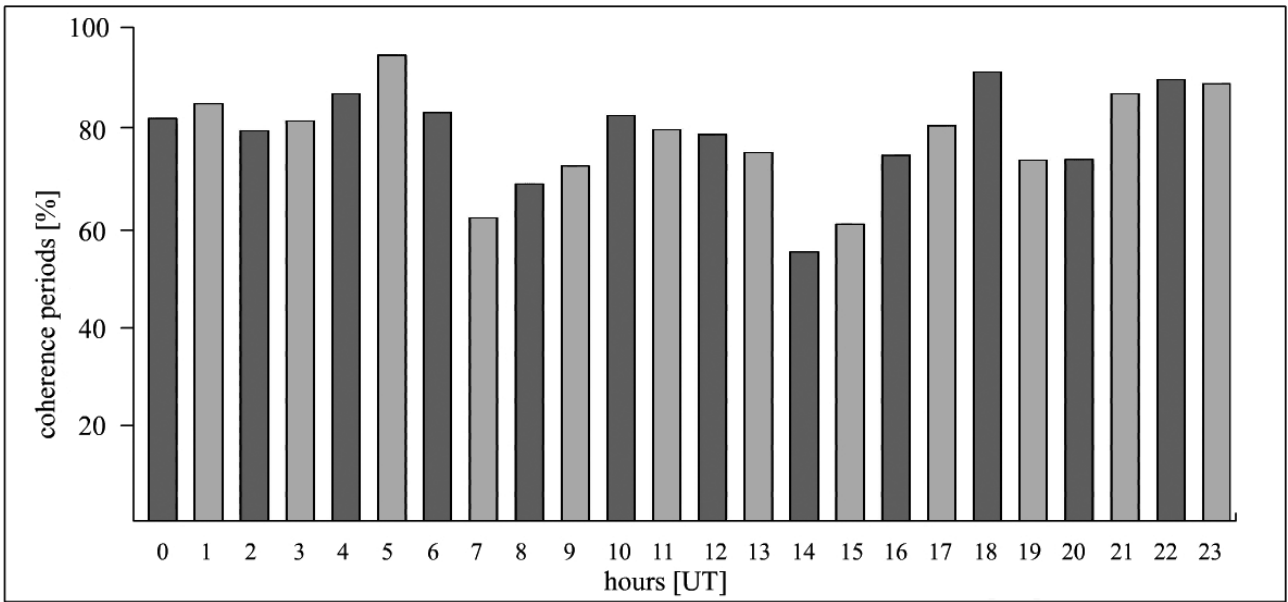

Figure 9. Percentage of occurrence of the periodicities at the various time intervals.

Figure 10. Percentages of occurrence of coherence for periods of 10-30 s calculated with the threshold values T_{dBm} = 1 dBm and $T_{h'}$ = 5 km.
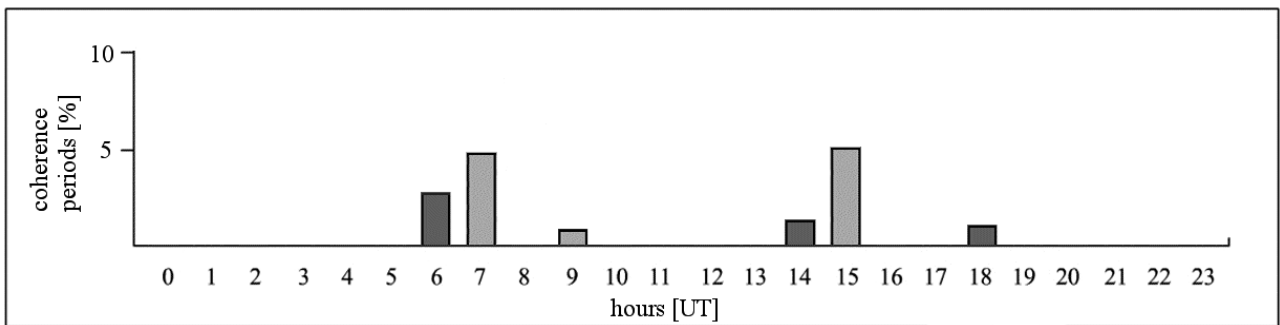

Figure 11. Percentage of occurrence of coherence for periods of 190-210 s calculated with the threshold values T_{dBm} = 1 dBm and $T_{h'}$ = 5 km.
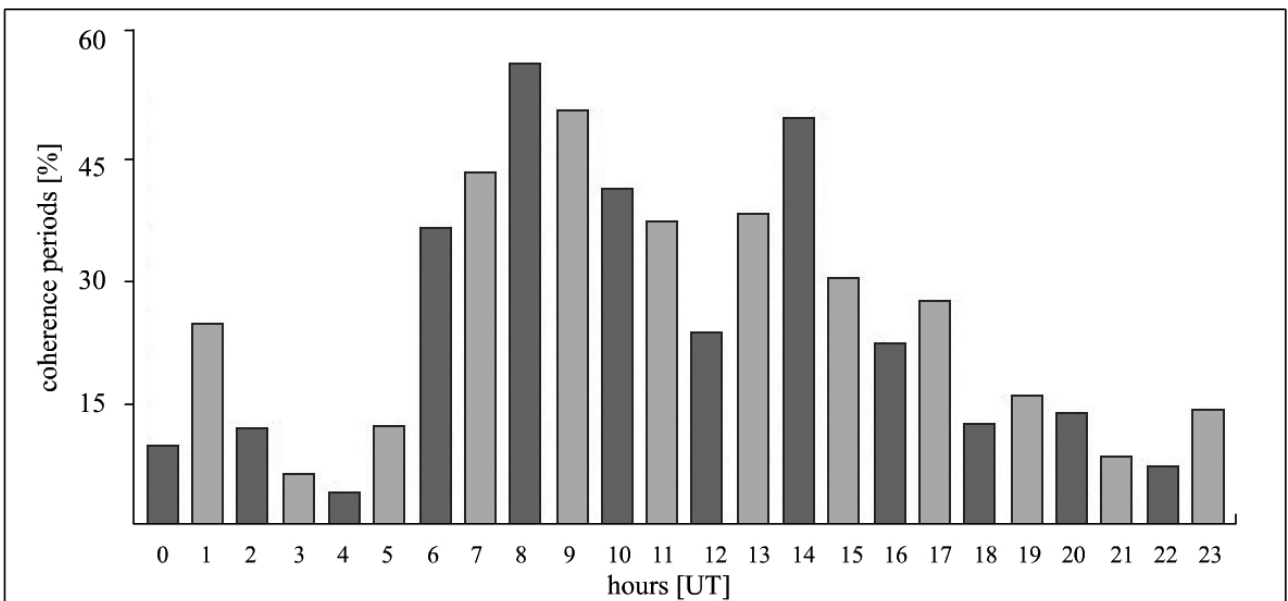

Figure 12. Percentage of occurrence of coherence for periods of 190-210 s calculated with the threshold values T_{dBm} = 5 dBm and $T_{h'}$ = 10 km.

pect is the determination of coherence time periods useful for remote sensing, radio, and OTH radar in order to maximize the coherent integration time.

The described results suggest that the propagation path trend, the multipath fading characteristics, and the time coherence of the ionospheric reflectors, are

mainly associated with SSD, which drive all these phenomena. The SSD are not predictable at least in the time-spatial scale considered in Table 2. The periodic analysis, limited to 512 s, showed that at this time scale of periodicity no pre-determined trend was observed and the fading follows a Rayleigh or a Nakagami-Rice trend, or a combination of them, with a predominance of the mixed case.

It has been found that the irregularities do not maintain a coherent motion for periods in the order of tens of seconds, while the prevalent periodicities are less than 25 s compatible with the SSD characteristics as illustrated in Table 2, and that the ionospheric reflector is characterized by periods of stability of 10-30 s for all the 24 hours.

References

Bianchi, C., U. Sciacca, E. Tabacco, A. Zirizzotti and E. Zuccheretti (2003). On the shape of reflecting surfaces investigated by a 60 MHz radar, Int. J. Remote Sens., 24 (15), 3049-3058.

Bianchi, C., J.A. Baskaradas, M. Pietrella, U. Sciacca and E. Zuccheretti (2013a). Power variation analysis of echo signals from ionospheric reflectors, Adv. Space Res., 51 (5), 722-729; http://dx.doi.org/10.1016/j.asr.2012.09.045.

Bianchi, C., J.A. Baskaradas, M. Pezzopane, M. Pietrella, U. Sciacca and E. Zuccheretti (2013b). Fading in the HF ionospheric channel and the role of irregularities, Adv. Space Res., 52 (3), 403-411; http://dx.doi.org/10.1016/j.asr.2013.03.035.

Blanc, E. (1985). Observations in the upper atmosphere of infrasonic waves from natural or artificial sources: A summary, Annales Geophysicae, 3, 673-688.

Crowley, G., and F.S. Rodrigues (2012). Characteristics of travelling ionospheric disturbances observed by the TIDDBIT sounder, Radio Science, 47, RS0L22; doi:10.1029/2011RS004959.

James, H.G., R.G. Gillies, G.C. Hussey and P. Prikryl (2006). HF fades caused by multiple wave fronts detected by a dipole antenna in the ionosphere, Radio Science, 41, RS4018; doi:10.1029/2005RS003385.

Krasnov, V.M., Y.V. Drobzheva and J. Lastovicka (2006). Recent advances and difficulties of infrasonic wave investigation in the ionosphere, Surv. Geophys., 27, 169-209; doi:10.1007/s10712-005-6203-4.

Leitinger, R., and M. Rieger (2005). The TID model for modulation of large scale electron density models, Annals of Geophysics, 48 (3), 515-523.

McNamara, L.F. (1991). The ionosphere: communications, surveillance, and direction finding, Krieger Pub. Co., 237 pp.

Nakagami, M. (1960). The m-distribution, a general formula of intensity distribution of rapid fading, In: W.C. Hoffman (ed.), Statistical Methods in Radio Wave Propagation, New York, Pergamon Press, 3-36.

Pietrella, M., and E. Zuccheretti (2010). Coerenza: A software tool for computing the maximum coherence times of the ionosphere, Computers & Geosciences, 36 (12), 1504-1511; doi:10.1016/j.cageo.2010.03.020.

Reinisch, B.W., and I. Galkin (2011). A Global Ionospheric Radio Observatory (GIRO), Earth Planets Space, 63, 377-381.

Rice, S.O. (1944). Mathematical analysis of random noise, Bell Systems Technological Journal, 23, 282-332.

Watterson, C.C., J.R. Juroshek and W.D. Bensema (1970). Experimental confirmation of an HF channel model, IEEE Transaction Communication Technology, COM-18, 792-803.

Yau, K.S.B., C.J. Coleman and M.A. Cervera (2006). Investigation on fading of high frequency radio signals propagating in the ionosphere - results from a Jindalee radar experiment, In: 10th IET International conference on ionospheric radio systems and techniques, IET Conference, Publication Issue CP517, 7-11.

Zuccheretti, E., G. Tutone, U. Sciacca, C. Bianchi and J.B. Arokiasamy (2003). The new AIS-INGV digital ionosonde, Annals of Geophysics, 46 (4), 647-659.

*Corresponding author: Umberto Sciacca,
Istituto Nazionale di Geofisica e Vulcanologia, Sezione Roma 1,
Rome, Italy; email: umberto.sciacca@ingv.it.